ARE ADVERSARIAL EXAMPLES INEVITABLE?

Ali Shafahi, W. Ronny Huang, Christoph Studer, Soheil Feizi, & Tom Goldstein

ABSTRACT

A wide range of defenses have been proposed to harden neural networks against adversarial attacks. However, a pattern has emerged in which the majority of adversarial defenses are quickly broken by new attacks. Given the lack of success at generating robust defenses, we are led to ask a fundamental question: Are adversarial attacks inevitable?

This paper analyzes adversarial examples from a theoretical perspective, and identifies fundamental bounds on the susceptibility of a classifier to adversarial attacks. We show that, for certain classes of problems, adversarial examples are inescapable. Using experiments, we explore the implications of theoretical guarantees for real-world problems and discuss how factors such as dimensionality and image complexity limit a classifier's robustness against adversarial examples.

1 INTRODUCTION

A number of adversarial attacks on neural networks have been recently proposed. To counter these attacks, a number of authors have proposed a range of defenses. However, these defenses are often quickly broken by new and revised attacks. Given the lack of success at generating robust defenses, we are led to ask a fundamental question: Are adversarial attacks inevitable?

In this paper, we identify a broad class of problems for which adversarial examples cannot be avoided. We also derive fundamental limits on the susceptibility of a classifier to adversarial attacks that depend on properties of the data distribution as well as the dimensionality of the dataset.

Adversarial examples occur when a small perturbation to an image changes its class label. There are different ways of measuring what it means for a perturbation to be "small"; as such, our analysis considers a range of different norms. While the ℓ_∞-norm is commonly used, adversarial examples can be crafted in any ℓ_p-norm (see Figure 1). We will see that the choice of norm can have a dramatic effect on the strength of theoretical guarantees for the existence of adversarial examples. Our analysis also extends to the ℓ_0-norm, which yields "sparse" adversarial examples that only perturb a small subset of image pixels (Figure 2).

As a simple example result, consider a classification problem with n-dimensional images with pixels scaled between 0 and 1 (in this case images live inside the unit hypercube). If the image classes each occupy a frac-

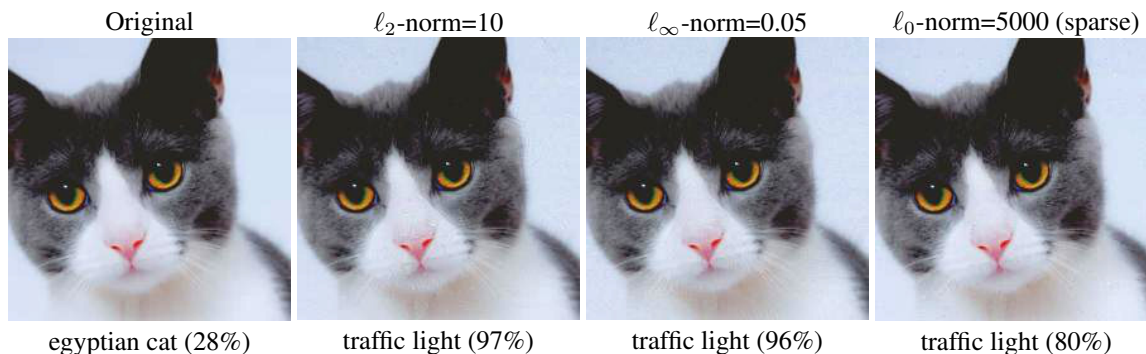| Original	ℓ_2-norm=10	ℓ_∞-norm=0.05	ℓ_0-norm=5000 (sparse)
egyptian cat (28%)	traffic light (97%)	traffic light (96%)	traffic light (80%)

Figure 1: Adversarial examples with different norm constraints formed via the projected gradient method (Madry et al., 2017) on Resnet50, along with the distance between the base image and the adversarial example, and the top class label.

tion of the cube greater than $\frac{1}{2}\exp(-\pi\epsilon^2)$, then images exist that are susceptible to adversarial perturbations of ℓ_2-norm at most ϵ. Note that $\epsilon = 10$ was used in Figure 1, and larger values are typical for larger images.

Finally, we discuss the validity of the presented guarantees for real-world datasets, and use experiments to explore whether these bounds accurately describe what we observe in practice.

1.1 BACKGROUND: A BRIEF HISTORY OF ADVERSARIAL EXAMPLES

Adversarial examples, first demonstrated in Szegedy et al. (2013) and Biggio et al. (2013), change the label of an image using small and often imperceptible perturbations to its pixels. A number of defenses have been proposed to harden networks against attacks, but historically, these defenses have been quickly broken. *Adversarial training*, one of the earliest defenses, successfully thwarted the fast gradient sign method (FGSM) (Goodfellow et al., 2014), one of the earliest and simplest attacks. However, adversarial training with FGSM examples was quickly shown to be vulnerable to more sophisticated multi-stage attacks (Kurakin et al., 2016; Tramèr et al., 2017a). More sophisticated defenses that rely on network distillation (Papernot et al., 2016b) and specialized activation functions (Zantedeschi et al., 2017) were also toppled by strong attacks (Papernot et al., 2016a; Tramèr et al., 2017b; Carlini & Wagner, 2016; 2017a).

The ongoing vulnerability of classifiers was highlighted in recent work by Athalye et al. (2018) and Athalye & Sutskever (2017) that broke an entire suite of defenses presented in ICLR 2018 including thermometer encoding (Buckman et al., 2018), detection using local intrinsic dimensionality (Ma et al., 2018), input transformations such as compression and image quilting (Guo et al., 2017), stochastic activation pruning (Dhillon et al., 2018), adding randomization at inference time (Xie et al., 2017), enhancing the confidence of image labels (Song et al., 2017), and using a generative model as a defense (Samangouei et al., 2018).

Rather than hardening classifiers to attacks, some authors have proposed sanitizing datasets to remove adversarial perturbations before classification. Approaches based on auto-encoders (Meng & Chen, 2017) and GANs (Shen et al., 2017) were broken using optimization-based attacks (Carlini & Wagner, 2017b;a).

A number of "certifiable" defense mechanisms have been developed for certain classifiers. Raghunathan et al. (2018) harden a two-layer classifier using semidefinite programming, and Sinha et al. (2018) propose a convex duality-based approach to adversarial training that works on sufficiently small adversarial perturbations with a quadratic adversarial loss. Kolter & Wong (2017) consider training a robust classifier using the convex outer adversarial polytope. All of these methods only consider robustness of the classifier on the training set, and robustness properties often fail to generalize reliably to test examples.

One place where researchers have enjoyed success is at training classifiers on low-dimensional datasets like MNIST (Madry et al., 2017; Sinha et al., 2018). The robustness achieved on more complicated datasets such as CIFAR-10 and ImageNet are nowhere near that of MNIST, which leads some researchers to speculate that adversarial defense is fundamentally harder in higher dimensions – an issue we address in Section 8.
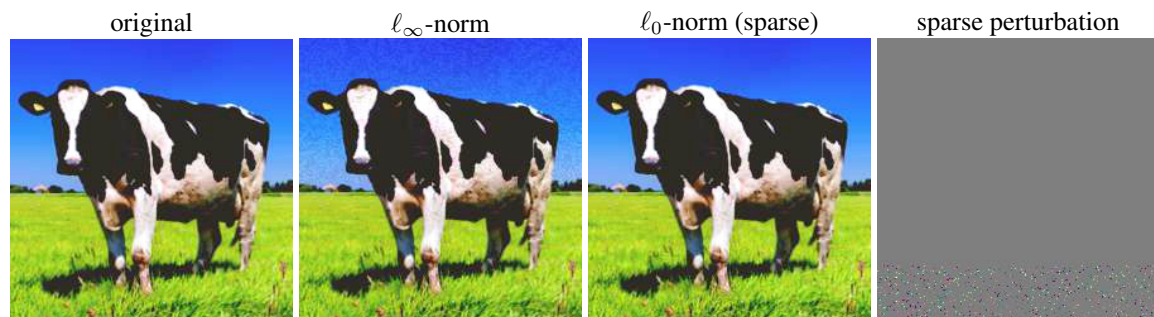

Figure 2: Sparse adversarial examples perturb a small subset of pixels and can hide adversarial "fuzz" inside high-frequency image regions. The original image (left) is classified as an "ox." Under ℓ_∞-norm perturbations, it is classified as "traffic light", but the perturbations visibly distort smooth regions of the image (the sky). These effects are hidden in the grass using ℓ_0-norm (sparse) perturbations limited to a small subset of pixels.

1.2 Notation

We use $[0, 1]^n$ to denote the unit hypercube in n dimensions, and $\text{vol}(\mathcal{A})$ to denote the volume (i.e., n-dimensional Lebesgue measure) of a subset $\mathcal{A} \subset [0, 1]^n$.

We use $\mathbb{S}^{n-1} = \{x \in \mathbb{R}^n \mid \|x\|_2 = 1\}$ to denote the unit sphere embedded in $\mathbb{R}^n$, and s_{n-1} to denote its surface area. The size of a subset $\mathcal{A} \in \mathbb{S}^{n-1}$ can be quantified by its ($n-1$ dimensional) measure $\mu[\mathcal{A}]$, which is simply the surface area the set covers. Because the surface area of the unit sphere varies greatly with n, it is much easier in practice to work with the *normalized measure*, which we denote $\mu_1[\mathcal{A}] = \mu[\mathcal{A}]/s_{n-1}$. This normalized measure has the property that $\mu_1[\mathbb{S}^{n-1}] = 1$, and so we can interpret $\mu_1[\mathcal{A}]$ as the probability of a uniform random point from the sphere lying in $\mathcal{A}$.

When we talk about the distance between points on a sphere, we frequently use the standard geodesic distance, which is always somewhat larger than (but comparable to) the Euclidean distance. In the cube, we measure distance between points using ℓ_p-norms, which are denoted

$$\|z\|_p = \left(\sum_i |z_i|^p \right)^{1/p} \text{ if } p > 0, \text{ and } \|z\|_0 = \text{card}\{z_i \mid z_i \neq 0\}.$$

Note that $\| \cdot \|_p$ is not truly a norm for $p < 1$, but rather a semi-norm. Such metrics are still commonly used, particularly the "ℓ_0-norm" which counts the number of non-zero entries in a vector.

2 Problem setup

We consider the problem of classifying data points that lie in a space Ω (either a sphere or a hypercube) into m different object classes. The m object classes are defined by probability density functions $\{\rho_c\}_{c=1}^m$, where $\rho_c : \Omega \to \mathbb{R}$. A "random" point from class c is a random variable with density ρ_c. We assume ρ_c to be bounded (i.e., we don't allow delta functions or other generalized functions), and denote its upper bound by $U_c = \sup_x \rho_c(x)$.

We also consider a "classifier" function $\mathcal{C} : \Omega \to \{1, 2, \ldots, m\}$ that partitions Ω into disjoint measurable subsets, one for each class label. The classifier we consider is discrete valued – it provides a label for each data point but not a confidence level.

With this setup, we can give a formal definition of an adversarial example.

Definition 1. *Consider a point $x \in \Omega$ drawn from class c, a scalar $\epsilon > 0$, and a metric d. We say that x admits an ϵ-adversarial example in the metric d if there exists a point $\hat{x} \in \Omega$ with $\mathcal{C}(\hat{x}) \neq c$, and $d(x, \hat{x}) \leq \epsilon$.*

In plain words, a point has an ϵ-adversarial example if we can sneak it into a different class by moving it at most ϵ units in the distance d.

We consider adversarial examples with respect to different ℓ_p-norm metrics. These metrics are written $d_p(x, \hat{x}) = \|x - \hat{x}\|_p$. A common choice is $p = \infty$, which limits the absolute change that can be made to any one pixel. However, ℓ_2-norm and ℓ_1-norm adversarial examples are also used, as it is frequently easier to create adversarial examples in these less restrictive metrics.

We also consider *sparse* adversarial examples in which only a small subset of pixels are manipulated. This corresponds to the metric d_0, in which case the constraint $\|x - \hat{x}\|_0 \leq \epsilon$ means that an adversarial example was crafted by changing at most ϵ pixels, and leaving the others alone.

3 The simple case: adversarial examples on the unit sphere

We begin by looking at the case of classifiers for data on the sphere. While this data model may be less relevant than the other models studied below, it provides a straightforward case where results can be proven using simple, geometric lemmas. The more realistic case of images with pixels in $[0, 1]$ will be studied in Section 4.
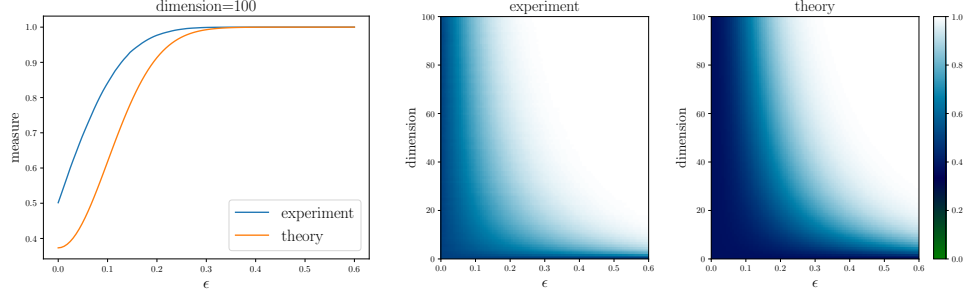
Figure 3: The ϵ-expansion of a half sphere nearly covers the whole sphere for small ϵ and large n. Visualizations show the fraction of the sphere captured within ϵ units of a half sphere in different dimensions. Results from a near-exact experimental method are compared to the theoretical lower bound in Lemma 2.

The idea is to show that, provided a class of data points takes up enough space, nearly every point in the class lies close to the class boundary. To show this, we begin with a simple definition.

Definition 2. *The ϵ-expansion of a subset $\mathcal{A} \in \Omega$ with respect to distance metric d, denoted $\mathcal{A}(\epsilon, d)$, contains all points that are at most ϵ units away from $\mathcal{A}$. To be precise*

$$\mathcal{A}(\epsilon, d) = \{x \in \Omega \mid d(x, y) \leq \epsilon \text{ for some } y \in \Omega\}.$$

We sometimes simply write $\mathcal{A}(\epsilon)$ when the distance metric is clear from context.

Our result provides bounds on the probability of adversarial examples that are independent of the shape of the class boundary. This independence is a simple consequence of an *isoperimetric inequality*. The classical isoperimetric inequality states that, of all closed surfaces that enclose a unit volume, the sphere has the smallest surface area. This simple fact is intuitive but famously difficult to prove. For a historical review of the isoperimetric inequality and its variants, see Osserman et al. (1978). We will use a special variant of the isoperimetric inequality first proved by Lévy & Pellegrino (1951) and simplified by Talagrand (1995).

Lemma 1 (Isoperimetric inequality). *Consider a subset of the sphere $\mathcal{A} \in \mathbb{S}^{n-1} \in \mathbb{R}^n$ with normalized measure $\mu_1(\mathcal{A}) = 1/2$. When using the geodesic metric, the ϵ-expansion $\mathcal{A}(\epsilon)$ is at least as large as the ϵ-expansion of a half sphere.*

The classical isoperimetric inequality is a simple geometric statement, and frequently appears without absolute bounds on the size of the ϵ-expansion of a half-sphere, or with bounds that involve unspecified constants (Vershynin, 2017). A tight bound derived by Milman & Schechtman (1986) is given below. The asymptotic blow-up of the ϵ-expansion of a half sphere predicted by this bound is shown in Figure 3.

Lemma 2 (ϵ-expansion of half sphere). *The geodesic ϵ-expansion of a half sphere has normalized measure at least*

$$1 - \left(\frac{\pi}{8}\right)^{\frac{1}{2}} \exp\left(-\frac{n-1}{2}\epsilon^2\right).$$

Lemmas 1 and 2 together can be taken to mean that, if a set isn't too small, then in high dimensions almost all points on the sphere are reachable within a short ϵ jump from that set. These lemmas have immediate implications for adversarial examples, which are formed by mapping one class into another using small perturbations. Despite its complex appearance, the result below is a consequence of the (relatively simple) isoperimetric inequality.

Theorem 1 (Existence of Adversarial Examples). *Consider a classification problem with m object classes, each distributed over the unit sphere $\mathbb{S}^{n-1} \in \mathbb{R}^n$ with density functions $\{\rho_c\}_{c=1}^m$. Choose a classifier function $\mathcal{C} : \mathbb{S}^{n-1} \to \{1, 2, \ldots, m\}$ that partitions the sphere into disjoint measurable subsets. Define the following scalar constants:*

- *Let V_c denote the magnitude of the supremum of ρ_c relative to the uniform density. This can be written $V_c := s_{n-1} \cdot \sup_x \rho_c(x)$.*
- *Let $f_c = \mu_1\{x | \mathcal{C}(x) = c\}$ be the fraction of the sphere labeled as c by classifier $\mathcal{C}$.*

4

Choose some class c with $f_c \leq \frac{1}{2}$. Sample a random data point x from ρ_c. Then with probability at least

$$1 - V_c \left(\frac{\pi}{8}\right)^{\frac{1}{2}} \exp\left(-\frac{n-1}{2}\epsilon^2\right) \tag{1}$$

one of the following conditions holds:

1. *x is misclassified by $\mathcal{C}$, or*
2. *x admits an ϵ-adversarial example in the geodesic distance.*

Proof. Choose a class c with $f_c \leq \frac{1}{2}$. Let $\mathcal{R} = \{x | \mathcal{C}(x) = c\}$ denote the region of the sphere labeled as class c by $\mathcal{C}$, and let $\overline{\mathcal{R}}$ be its complement. $\overline{\mathcal{R}}(\epsilon)$ is the ϵ-expansion of $\overline{\mathcal{R}}$ in the geodesic metric. Because $\overline{\mathcal{R}}$ covers at least half the sphere, the isoperimetric inequality (Lemma 1) tells us that the epsilon expansion is at least as great as the epsilon expansion of a half sphere. We thus have

$$\mu_1[\overline{R}(\epsilon)] \geq 1 - \left(\frac{\pi}{8}\right)^{\frac{1}{2}} \exp\left(-\frac{n-1}{2}\epsilon^2\right).$$

Now, consider the set $\mathcal{S}_c$ of "safe" points from class c that are correctly classified and do not admit adversarial perturbations. A point is correctly classified only if it lies inside $\mathcal{R}$, and therefore outside of $\overline{\mathcal{R}}$. To be safe from adversarial perturbations, a point cannot lie within ϵ distance from the class boundary, and so it cannot lie within $\overline{R}(\epsilon)$. It is clear that the set $\mathcal{S}_c$ of safe points is exactly the complement of $\overline{R}(\epsilon)$. This set has normalized measure

$$\mu_1[\mathcal{S}_c] \leq \left(\frac{\pi}{8}\right)^{\frac{1}{2}} \exp\left(-\frac{n-1}{2}\epsilon^2\right).$$

The probability of a random point lying in $\mathcal{S}_c$ is bounded above by the normalized supremum of ρ_c times the normalized measure $\mu_1[\mathcal{S}_c]$. This product is given by

$$V_c \left(\frac{\pi}{8}\right)^{\frac{1}{2}} \exp\left(-\frac{n-1}{2}\epsilon^2\right).$$

We then subtract this probability from 1 to obtain the probability of a point lying outside the safe region, and arrive at equation 1. $\qquad\square$

In the above result, we measure the size of adversarial perturbations using the geodesic distance. Most studies of adversarial examples measure the size of perturbation in either the ℓ_2 (Euclidean) norm or the ℓ_∞ (max) norm, and so it is natural to wonder whether Theorem 1 depends strongly on the distance metric. Fortunately (or, rather unfortunately) it does not.

It is easily observed that, for any two points x and y on a sphere,

$$d_\infty(x, y) \leq d_2(x, y) \leq d_g(x, y),$$

where $d_\infty(x, y)$, $d_2(x, y)$, and $d_g(x, y)$ denote the l_∞, Euclidean, and geodesic distance, respectively. From this, we see that Theorem 1 is actually fairly conservative; any ϵ-adversarial example in the geodesic metric would also be adversarial in the other two metrics, and the bound in Theorem 1 holds regardless of which of the three metrics we choose (although different values of ϵ will be appropriate depending on the norm).

4 WHAT ABOUT THE UNIT CUBE?

The above result about the sphere is simple and easy to prove using classical results. However, real world images do not lie on the sphere. In a more typical situation, images will be scaled so that their pixels lie in $[0, 1]$, and data lies inside a high-dimensional hypercube (but, unlike the sphere, data is not confined to its surface). The proof of Theorem 1 makes extensive use of properties that are exclusive to the sphere, and is not applicable to this more realistic setting. Are there still problem classes on the cube where adversarial examples are inevitable?

This question is complicated by the fact that simple, geometric isoperimetric inequalities fail to exist for the cube, and the shapes that achieve minimal ϵ-expansion (if they exist) depend on the volume they enclose and the choice of ϵ. Fortunately, it is still possible to derive "algebraic" isoperimetric inequalities that provide lower bounds on the size of the ϵ-expansion of sets without identifying the shape that achieves this minimum. The proof of this result is in Appendix A.

Lemma 3 (Isoperimetric inequality on a cube). *Consider a measurable subset of the cube $\mathcal{A} \subset [0, 1]^n$, and a p-norm distance metric $d_p(x, y) = \|x - y\|_p$ for $p > 0$. Let $\Phi(z) = (2\pi)^{-\frac{1}{2}} \int_{-\infty}^{z} e^{-t^2/2} dt$, and let α be the scalar that satisfies $\Phi(\alpha) = \text{vol}[\mathcal{A}]$. Then*

$$\text{vol}[\mathcal{A}(\epsilon, d_p)] \geq \Phi\left(\alpha + \frac{\sqrt{2\pi n}}{n^{1/p^*}} \epsilon\right) \tag{2}$$

where $p^* = \min(p, 2)$. In particular, if $\text{vol}(\mathcal{A}) \geq 1/2$, then we simply have

$$\text{vol}[\mathcal{A}(\epsilon, d_p)] \geq 1 - \frac{\exp(-\pi n^{1-2/p^*} \epsilon^2)}{2\pi n^{1/2-1/p^*}}. \tag{3}$$

Using this result, we can show that most data samples in a cube admit adversarial examples, provided the data distribution is not excessively concentrated.

Theorem 2 (Adversarial examples on the cube). *Consider a classification problem with m classes, each distributed over the unit hypercube $[0, 1]^n$ with density functions $\{\rho_c\}_{c=1}^m$. Choose a classifier function $\mathcal{C} : [0, 1]^n \to \{1, 2, \ldots, m\}$ that partitions the hypercube into disjoint measurable subsets. Define the following scalar constants:*

- *Let U_c denote the supremum of ρ_c.*
- *Let f_c be the fraction of hypercube partitioned into class c by $\mathcal{C}$.*

Choose some class c with $f_c \leq \frac{1}{2}$, and select an ℓ_p-norm with $p > 0$. Define $p^* = \min(p, 2)$. Sample a random data point x from the class distribution ρ_c. Then with probability at least

$$1 - U_c \frac{\exp(-\pi n^{1-2/p^*} \epsilon^2)}{2\pi n^{1/2-1/p^*}}. \tag{4}$$

one of the following conditions holds:

1. *x is misclassified by $\mathcal{C}$, or*
2. *x has an adversarial example $\hat{x}$, with $\|x - \hat{x}\|_p \leq \epsilon$.*

When adversarial examples are defined in the ℓ_2-norm, the bound in equation 4 has the simple form

$$1 - U_c \exp(-\pi\epsilon^2)/(2\pi). \tag{5}$$

Provided the class distribution is not overly concentrated, Theorem 5 guarantees adversarial examples with relatively "small" ϵ relative to a typical vector. In n dimensions, the ℓ_2 diameter of the cube is $\sqrt{n}$, and so it is reasonable to choose $\epsilon = O(\sqrt{n})$ in equation 5. In Figure 1, we chose $\epsilon = 10$. A similarly strong bound of $1 - U_c\sqrt{n}\exp(-\pi\epsilon^2/n)/(2\pi)$ holds for the case of the ℓ_1-norm, in which case the diameter is n.

Oddly, equation 4 seems particularly weak when the ℓ_∞ norm is used. In this case, the bound on the right side of equation 4 becomes equation 5 just like in the ℓ_2 case. However, ℓ_∞ adversarial examples are only interesting if we take $\epsilon < 1$, in which case equation 5 becomes vacuous for large n. This bound can be tightened up in certain situations. If we prove Theorem 2 using the tighter (but messier) bound of equation 2 instead of equation 3, we can replace equation 4 with

$$1 - U_c \hat{\Phi}\left(\alpha + \sqrt{2\pi}\epsilon\right)$$

for $p \geq 2$, where $\hat{\Phi}(z) = \frac{1}{\sqrt{2\pi}} \int_z^{\infty} e^{-t^2/2} dt \geq \frac{1}{\sqrt{2\pi}z} e^{-z^2/2}$ (for $z > 0$), and $\alpha = \Phi^{-1}(1 - f_c)$. For this bound to be meaningful with $\epsilon < 1$, we need f_c to be relatively small, and ϵ to be roughly f_c or smaller. This is realistic for some problems; ImageNet has 1000 classes, and so $f_c < 10^{-3}$ for at least one class.

One might wonder whether the weakness of Theorem 4 in the ℓ_∞ case is fundamental, or if this is simply a failure of our approach. It is possible to construct examples of sets with ℓ_∞ expansions that nearly match the behavior of equation 5, and so our theorems in this case are actually quite tight. It seems to be inherently more difficult to prove the existence of adversarial examples in the cube using the ℓ_∞-norm.

5 WHAT ABOUT SPARSE ADVERSARIAL EXAMPLES?

A number of papers have looked at *sparse* adversarial examples, in which a small number of image pixels, in some cases only one (Su et al., 2017), are changed to manipulate the class label. To study this case, we would like to investigate adversarial examples under the ℓ_0 metric. The ℓ_0 distance is defined as

$$d(x, y) = \|x - y\|_0 = \operatorname{card}\{i \mid x_i \neq y_i\}.$$

If a point x has an ϵ-adversarial example in this norm, then it can be perturbed into a different class by modifying at most ϵ pixels (in this case ϵ is taken to be a positive integer).

Theorem 2 is fairly tight for $p = 1$ or 2. However, the bound becomes quite loose for small p, and in particular it fails completely for the important case of $p = 0$. For this reason, we present a different bound that is considerably tighter for small p (although slightly looser for large p).

The case of $p = 0$ was first studied by Milman & Schechtman (1986) and McDiarmid (1989). However, results of this type are most commonly associated with Talagrand (1995; 1996) who used them to study a wide range of applications in probability, combinatorics, and optimization. The proof of the following theorem (which appears in the appendix) follows the method of Talagrand, with modifications made to extend the proof to arbitrary p by exploiting properties of the unit cube.

Note that the ℓ_p-norm is defined as $\|z\|_p = \left(\sum_i |z_i|^p\right)^{1/p}$ for $p > 0$, while the ℓ_0 "norm" is $\|z\|_0 = \lim_{p \to 0} \sum_i |z_i|^p$ (notice the lack of a $1/p$ exponent around the sum). The result below addresses the ℓ_0 norm separately to deal with this inconsistency of notation.

Lemma 4 (Isoperimetric inequality on the cube: small p). *Consider a measurable subset of the cube $\mathcal{A} \subset [0, 1]^n$, and a p-norm distance metric $d(x, y) = \|x - y\|_p$ for any $p \geq 0$. We have*

$$\operatorname{vol}[\mathcal{A}(\epsilon, d_p)] \geq 1 - \frac{\exp\left(-\epsilon^{2p}/n\right)}{\operatorname{vol}[\mathcal{A}]}, \textit{ for } p > 0 \textit{ and} \tag{6}$$

$$\operatorname{vol}[\mathcal{A}(\epsilon, d_0)] \geq 1 - \frac{\exp\left(-\epsilon^{2}/n\right)}{\operatorname{vol}[\mathcal{A}]}, \textit{ for } p = 0. \tag{7}$$

Using this result, we can prove a statement analogous to Theorem 2, but for sparse adversarial examples. We present only the case of $p = 0$, but the generalization to the case of other small p using Lemma 4 is straightforward.

Theorem 3 (Sparse adversarial examples). *Consider the problem setup of Theorem 2. Choose some class c with $f_c \leq \frac{1}{2}$, and sample a random data point x from the class distribution ρ_c. Then with probability at least*

$$1 - 2U_c \exp(-\epsilon^2/n) \tag{8}$$

one of the following conditions holds:

1. *x is misclassified by $\mathcal{C}$, or*

2. *x can be adversarially perturbed by modifying at most ϵ pixels, while still remaining in the unit hypercube.*

6 WHAT IF WE JUST SHOW THAT ADVERSARIAL EXAMPLES EXIST?

Tighter bounds can be obtained if we only guarantee that adversarial examples exist for *some* data points in a class, without bounding the probability of this event.

Theorem 4 (Condition for existence of adversarial examples)**.** *Consider the setup of Theorem 2. Choose a class c that occupies a fraction of the cube $f_c < \frac{1}{2}$. Pick an ℓ_p norm and set $p^* = \min(p, 2)$.*

Let $\mathrm{supp}(\rho_c)$ denote the support of ρ_c. Then there is a point x with $\rho_c(x) > 0$ that admits an ϵ-adversarial example if

$$\mathrm{vol}[\mathrm{supp}(\rho_c)] \geq \begin{cases} \frac{1}{2}\exp(-\pi\epsilon^2 n^{1-2/p^*}), & \text{for } p > 0 \text{ or} \\ \exp\left(-2\left(\epsilon - \sqrt{\frac{n\log 2}{2}}\right)^2 / n\right), & \text{for } p = 0. \end{cases} \tag{9}$$

The bound for the case $p = 0$ is valid only if $\epsilon \geq \sqrt{n \log 2/2}$.

It is interesting to consider when Theorem 4 produces non-vacuous bounds. When the ℓ_2-norm is used, the bound becomes $\mathrm{vol}[\mathrm{supp}(\rho_c)] \geq \exp(-\pi\epsilon^2)/2$. The diameter of the cube is $\sqrt{n}$, and so the bound becomes active for $\epsilon = \sqrt{n}$. Plugging this in, we see that the bound is active whenever the size of the support satisfies

$$\mathrm{vol}[\mathrm{supp}(\rho_c)] > \frac{1}{2e^{\pi n}}.$$

Remarkably, this holds for large n whenever the support of class c is larger than (or contains) a hypercube of side length at least $e^{-\pi} \approx 0.043$.

7 DISCUSSION: CAN WE ESCAPE FUNDAMENTAL BOUNDS?

There are a number of ways to escape the guarantees of adversarial examples made by Theorems 1-4. Here, we address a variety of ways that classifiers could escape these bounds. One potential escape is for the class density functions to take on extremely large values (i.e., exponentially large U_c); the dependence of U_c on n is addressed separately in Section 8.

Unbounded density functions and low-dimensional data manifolds In practice, image datasets might lie on low-dimensional manifolds within the cube, and the support of these distributions could have measure zero, making the density function infinite (i.e., $U_c = \infty$). The arguments above are still relevant in this case; we can expand the data manifold by adding a uniform random noise to each image pixel of magnitude at most $\epsilon/2$. The expanded dataset has positive volume. Then, adversarial examples of this expanded dataset can be crafted with perturbations of size $\epsilon/2$. These adversarial examples will lie at most ϵ units away from the original (low-dimensional) dataset. We saw in Section 6 that adding a uniform noise on $[-e^{-\pi}/2, e^{-\pi}/2] \approx [-0.022, 0.022]$ to each pixel is already enough to provide a meaningful bound.

This method of expanding the manifold before crafting adversarial examples is often used in practice. Tramèr et al. (2017a) proposed adding a small $\epsilon/2$ perturbation to step off the image manifold before crafting adversarial examples. This strategy is also used during adversarial training (Madry et al., 2017).

Adding a "don't know" class The analysis above assumes the classifier assigns a label to every point in the cube. If a classifier has the ability to say "I don't know," rather than assign a label to every input, then the region of the cube that is assigned class labels might be very small, and adversarial examples could be escaped even if the other assumptions of Theorem 4 are satisfied. In this case, it would still be easy for the adversary degrade classifier performance by perturbing images into the "don't know" class.

Feature squeezing Provided that decreasing the dimensionality of the dataset does not lead to substantially increased values for U_c (we see in Section 8 that this is a reasonable assumption), measuring data in lower dimensions could result in a classifier that is more difficult to manipulate. Note, however, that decreasing resolution only avoids the bounds in Theorems 1-4 if images are *acquired* at the lower resolution. If the adversary provides images at higher resolution which are then feature squeezed via an auto-encoder (Meng & Chen, 2017; Shen et al., 2017), JPEG encoding (Das et al., 2018), or quantization (Xu et al., 2017) as part of the classification process, then the classifier is still subject to the bound at the higher resolution.

Computational hardness It may be computationally hard to craft adversarial examples because of local flatness of the classification function, obscurity of the classifier function, or other computational difficulties. Computational hardness could prevent adversarial attacks in practice, even if adversarial examples still exist.

8 Experiments & Effect of Dimensionality

In this section, we discuss the relationship between dimensionality and adversarial robustness, and explore how the predictions made by the theorems above are reflected in experiments.

It is commonly thought that high-dimensional classifiers are more susceptible to adversarial examples than low-dimensional classifiers. This perception is partially motivated by the observation that classifiers on high-resolution image distributions like ImageNet are more easily fooled than low resolution classifiers on MNIST (Tramèr et al., 2017a). Indeed, Theorem 2 predicts that high-dimensional classifiers should be much easier to fool than low-dimensional classifiers, assuming the datasets they classify have comparable probability density limits U_c. However, this is not a reasonable assumption; we will see below that high dimensional distributions may be more concentrated than their low-dimensional counterparts.

We study the effects of dimensionality with a thought experiment involving a "big MNIST" image distribution. Given an integer expansion factor b, we can make a big MNIST distribution, denoted b-MNIST, by replacing each pixel in an MNIST image with a $b \times b$ array of identical pixels. This expands an original 28×28 image into a $28b \times 28b$ image. Figure 4a shows that, without adversarial training, a classifier on big MNIST is far more susceptible to attacks than a classifier trained on the original MNIST[1].

However, each curve in Figure 4a only shows the attack susceptibility of one particular classifier. In contrast, Theorems 1-4 describe the *fundamental* limits of susceptibility for all classifiers. These limits are an inherent property of the data distribution. The theorem below shows that these fundamental limits *do not* depend in a non-trivial way on the dimensionality of the images in big MNIST, and so the relationship between dimensionality and susceptibility in Figure 4a results from the weakness of the training process.

Theorem 5. *Suppose ϵ and p are such that, for all MNIST classifiers, a random image from class c has an ϵ-adversarial example (in the ℓ_2-norm) with probability at least p. Then for all classifiers on b-MNIST, a random image from c has a $b\epsilon$-adversarial example with probability at least p.*

Likewise, if all b-MNIST classifiers have $b\epsilon$-adversarial examples with probability p, then all classifiers on the original MNIST distribution have ϵ-adversarial examples with probability p.

Theorem 5 predicts that the perturbation needed to fool all 56×56 classifiers is twice that needed to fool all 28×28 classifiers. This is reasonable since the ℓ_2-norm of a 56×56 image is twice that of its 28×28 counterpart. Put simply, fooling big MNIST is just as hard/easy as fooling the original MNIST regardless of resolution. It also shows that for big MNIST, as the expansion factor b gets larger and ϵ is expanded to match, the concentration bound U_c grows at exactly the same rate as the exponential term in equation 2 shrinks, and there is no net effect on fundamental susceptibility. Also note that an analogous result could be based on any image classification problem (we chose MNIST only for illustration), and any $p \geq 0$.

We get a better picture of the fundamental limits of MNIST by considering classifiers that are hardened by adversarial training[2] (Figure 4b). These curves display several properties of fundamental limits predicted by our theorems. As predicted by Theorem 5, the 112×112 classifer curve is twice as wide as the 56×56 curve, which in turn is twice as wide as the 28×28 curve. In addition, we see the kind of "phase transition" behavior predicted by Theorem 2, in which the classifier suddenly changes from being highly robust to being highly susceptible as ϵ passes a critical threshold. For these reasons, it is reasonable to suspect that the adversarially trained classifiers in Figure 4b are operating near the fundamental limit predicted by Theorem 2.

Theorem 5 shows that increased dimensionality does not increase adversarial susceptibility in a fundamental way. But then why are high-dimensional classifiers so easy to fool? To answer this question, we look at the concentration bound U_c for object classes. The smallest possible value of U_c is 1, which only occurs when image pixels are uniform and *uncorrelated*. In contrast, adjacent pixels in MNIST (and especially big MNIST) are very highly correlated, resulting in highly concentrated image classes with large U_c. Theory predicts that such highly concentrated datasets can be relatively safe from adversarial examples.

---

[1] All classifiers have the same number of convolutional layers and filters. Only the fully-connected layer is modified to handle the difference in dimensionality between datasets.

[2] Adversarial examples for MNIST and CIFAR-10 were produced as in Madry et al. (2017) using a 100-step and 20-step projected gradient method.
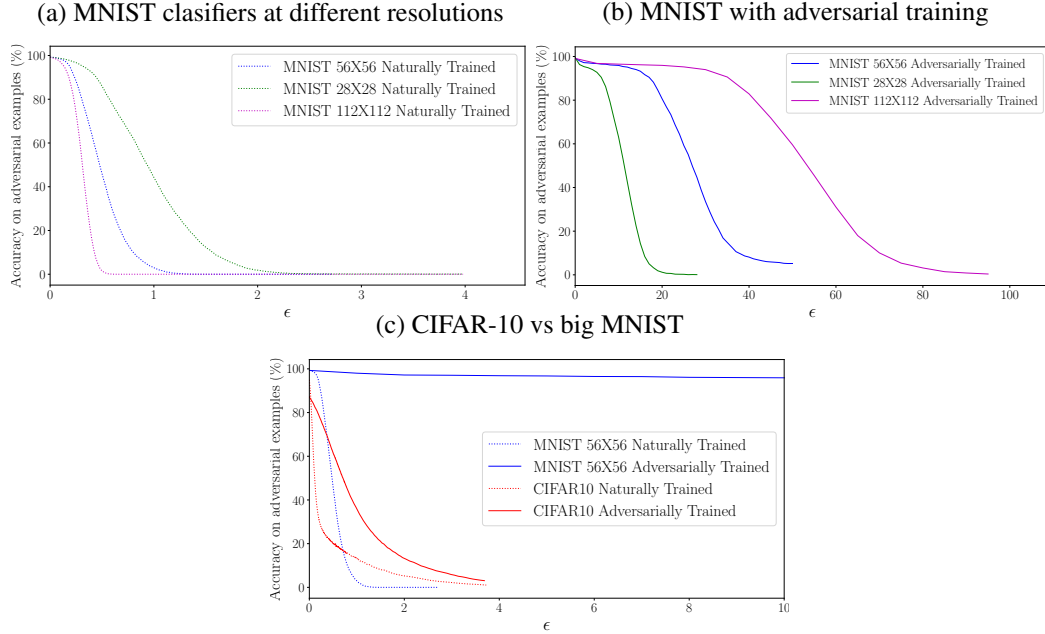
(a) MNIST clasifiers at different resolutions

(b) MNIST with adversarial training

(c) CIFAR-10 vs big MNIST

Figure 4: (a) The attack susceptibilities of MNIST and "big" MNIST classifiers are plotted as a function of ϵ. The susceptibility of naturally trained classifiers worsens with increased dimensionality. (b) When adversarial training is used, the susceptibility curves behave like the fundamental limits predicted by Theorems 2 and 5. (c) The susceptibility of CIFAR-10 is compared to big MNIST. Both datasets have similar numbers of features, but the higher complexity of CIFAR-10 results in far worse susceptibility. All perturbations are measured in the ℓ_2-norm.

We can reduce U_c and dramatically increase susceptibility by choosing a more "spread out" dataset, like CIFAR-10, in which adjacent pixels are less strongly correlated. We observe the effect of decreasing U_c by plotting the susceptibility of a 56×56 MNIST classifier against a classifier for CIFAR-10 (Figure 4, right). The former problem lives in 3136 dimensions, while the latter lives in 3072, and both have 10 classes. Despite the structural similarities between these problems, the decreased concentration of CIFAR-10 results in vastly more susceptibility to attacks, regardless of whether adversarial training is used. The theory above suggests that this increased susceptibility is caused (at least in part) by a shift in the fundamental limits for CIFAR-10, rather than the weakness of the particular classifiers we chose.

Intuitively, the concentration limit U_c can be interpreted as a measure of image *complexity*. Image classes with smaller U_c likely have weaker correlations between pixels, more intra-class variation, and thus more apparent complexity. Theorem 2 shows that "high complexity" image classes are fundamentally more susceptible to adversarial examples, and Figure 4 suggests that complexity (rather than dimensionality) is largely responsible for differences we observe in the effectiveness of adversarial training for different datasets.

9 CONCLUSION

Any classification problem has a fundamental limit on robustness to adversarial attacks that cannot be escaped by any classifier. This paper provides a characterization of these limits and how they depend on properties of the data distribution. Unfortunately, it is impossible to know the exact properties of real-world image distributions or the resulting fundamental limits of adversarial training for arbitrary datasets. However, the analysis and experiments in this paper suggest that, especially for complex image classes in high-dimensional spaces, these limits may be far worse than our intuition tells us.

10

10 Acknowledgements

References

Milton Abramowitz and Irene A Stegun. *Handbook of mathematical functions: with formulas, graphs, and mathematical tables*, volume 55. Courier Corporation, 1965.

Anish Athalye and Ilya Sutskever. Synthesizing robust adversarial examples. *arXiv preprint arXiv:1707.07397*, 2017.

Anish Athalye, Nicholas Carlini, and David Wagner. Obfuscated gradients give a false sense of security: Circumventing defenses to adversarial examples. *arXiv preprint arXiv:1802.00420*, 2018.

Battista Biggio, Igino Corona, Davide Maiorca, Blaine Nelson, Nedim Šrndić, Pavel Laskov, Giorgio Giacinto, and Fabio Roli. Evasion attacks against machine learning at test time. In *Joint European conference on machine learning and knowledge discovery in databases*, pp. 387–402. Springer, 2013.

Sergey G Bobkov et al. An isoperimetric inequality on the discrete cube, and an elementary proof of the isoperimetric inequality in gauss space. *The Annals of Probability*, 25(1):206–214, 1997.

Jacob Buckman, Aurko Roy, Colin Raffel, and Ian Goodfellow. Thermometer encoding: One hot way to resist adversarial examples. *OpenReview*, 2018.

Nicholas Carlini and David Wagner. Defensive distillation is not robust to adversarial examples. *arXiv preprint arXiv:1607.04311*, 2016.

Nicholas Carlini and David Wagner. Magnet and "efficient defenses against adversarial attacks" are not robust to adversarial examples. *arXiv preprint arXiv:1711.08478*, 2017a.

Nicholas Carlini and David Wagner. Towards evaluating the robustness of neural networks. In *Security and Privacy (SP), 2017 IEEE Symposium on*, pp. 39–57. IEEE, 2017b.

Nilaksh Das, Madhuri Shanbhogue, Shang-Tse Chen, Fred Hohman, Siwei Li, Li Chen, Michael E Kounavis, and Duen Horng Chau. Shield: Fast, practical defense and vaccination for deep learning using JPEG compression. *arXiv preprint arXiv:1802.06816*, 2018.

Guneet S Dhillon, Kamyar Azizzadenesheli, Zachary C Lipton, Jeremy Bernstein, Jean Kossaifi, Aran Khanna, and Anima Anandkumar. Stochastic activation pruning for robust adversarial defense. *arXiv preprint arXiv:1803.01442*, 2018.

Ian J Goodfellow, Jonathon Shlens, and Christian Szegedy. Explaining and harnessing adversarial examples. *arXiv preprint arXiv:1412.6572*, 2014.

Chuan Guo, Mayank Rana, Moustapha Cisse, and Laurens van der Maaten. Countering adversarial images using input transformations. *arXiv preprint arXiv:1711.00117*, 2017.

J Zico Kolter and Eric Wong. Provable defenses against adversarial examples via the convex outer adversarial polytope. *arXiv preprint arXiv:1711.00851*, 2017.

Alexey Kurakin, Ian Goodfellow, and Samy Bengio. Adversarial examples in the physical world. *arXiv preprint arXiv:1607.02533*, 2016.

Paul Lévy and Franco Pellegrino. *Problémes concrets d'analyse fonctionnelle*. Gauthier-Villars, Paris, 1951.

Xingjun Ma, Bo Li, Yisen Wang, Sarah M Erfani, Sudanthi Wijewickrema, Michael E Houle, Grant Schoenebeck, Dawn Song, and James Bailey. Characterizing adversarial subspaces using local intrinsic dimensionality. *arXiv preprint arXiv:1801.02613*, 2018.

Aleksander Madry, Aleksandar Makelov, Ludwig Schmidt, Dimitris Tsipras, and Adrian Vladu. Towards deep learning models resistant to adversarial attacks. *arXiv preprint arXiv:1706.06083*, 2017.

C McDiarmid. On the method of bounded differences. *London Mathematical Society Lecture Notes*, 141: 148–188, 1989.

Dongyu Meng and Hao Chen. MagNet: a two-pronged defense against adversarial examples. In *Proceedings of the 2017 ACM SIGSAC Conference on Computer and Communications Security*, pp. 135–147. ACM, 2017.

Vitali D Milman and Gideon Schechtman. *Asymptotic Theory of Finite Dimensional Normed Spaces*. Springer-Verlag, Berlin, Heidelberg, 1986. ISBN 0-387-16769-2.

Robert Osserman et al. The isoperimetric inequality. *Bulletin of the American Mathematical Society*, 84(6): 1182–1238, 1978.

Nicolas Papernot, Patrick McDaniel, and Ian Goodfellow. Transferability in machine learning: from phenomena to black-box attacks using adversarial samples. *arXiv preprint arXiv:1605.07277*, 2016a.

Nicolas Papernot, Patrick McDaniel, Xi Wu, Somesh Jha, and Ananthram Swami. Distillation as a defense to adversarial perturbations against deep neural networks. In *Security and Privacy (SP), 2016 IEEE Symposium on*, pp. 582–597. IEEE, 2016b.

Aditi Raghunathan, Jacob Steinhardt, and Percy Liang. Certified defenses against adversarial examples. *arXiv preprint arXiv:1801.09344*, 2018.

Pouya Samangouei, Maya Kabkab, and Rama Chellappa. Defense-GAN: Protecting classifiers against adversarial attacks using generative models. *arXiv preprint arXiv:1805.06605*, 2018.

Shiwei Shen, Guoqing Jin, Ke Gao, and Yongdong Zhang. APE-GAN: Adversarial perturbation elimination with GAN. *ICLR Submission, available on OpenReview*, 4, 2017.

Aman Sinha, Hongseok Namkoong, and John Duchi. Certifying some distributional robustness with principled adversarial training. *OpenReview*, 2018.

Yang Song, Taesup Kim, Sebastian Nowozin, Stefano Ermon, and Nate Kushman. PixelDefend: Leveraging generative models to understand and defend against adversarial examples. *arXiv preprint arXiv:1710.10766*, 2017.

Jiawei Su, Danilo Vasconcellos Vargas, and Sakurai Kouichi. One pixel attack for fooling deep neural networks. *arXiv preprint arXiv:1710.08864*, 2017.

Vladimir Sudakov and Boris Tsirelson. Extremal properties of half-spaces for spherically invariant measures. *J. Soviet Math.*, 41, 1974.

Christian Szegedy, Wojciech Zaremba, Ilya Sutskever, Joan Bruna, Dumitru Erhan, Ian Goodfellow, and Rob Fergus. Intriguing properties of neural networks. *arXiv preprint arXiv:1312.6199*, 2013.

Michel Talagrand. Concentration of measure and isoperimetric inequalities in product spaces. *Publications Mathématiques de l'Institut des Hautes Etudes Scientifiques*, 81(1):73–205, 1995.

Michel Talagrand. A new look at independence. *The Annals of probability*, pp. 1–34, 1996.

Florian Tramèr, Alexey Kurakin, Nicolas Papernot, Ian Goodfellow, Dan Boneh, and Patrick McDaniel. Ensemble adversarial training: Attacks and defenses. *arXiv preprint arXiv:1705.07204*, 2017a.

Florian Tramèr, Nicolas Papernot, Ian Goodfellow, Dan Boneh, and Patrick McDaniel. The space of transferable adversarial examples. *arXiv preprint arXiv:1704.03453*, 2017b.

Roman Vershynin. *High-Dimensional Probability*. Cambridge University Press, 2017.

Cihang Xie, Jianyu Wang, Zhishuai Zhang, Zhou Ren, and Alan Yuille. Mitigating adversarial effects through randomization. *arXiv preprint arXiv:1711.01991*, 2017.

Weilin Xu, David Evans, and Yanjun Qi. Feature squeezing: Detecting adversarial examples in deep neural networks. *arXiv preprint arXiv:1704.01155*, 2017.

Valentina Zantedeschi, Maria-Irina Nicolae, and Ambrish Rawat. Efficient defenses against adversarial attacks. In *Proceedings of the 10th ACM Workshop on Artificial Intelligence and Security*, pp. 39–49. ACM, 2017.

A   PROOF OF LEMMA 3

We now prove Lemma 3. To do this, we being with a classical isoperimetric inequality for random Gaussian variables. Unlike the case of a cube, tight geometric isoperimetric inequalities exist in this case. We then prove results about the cube by creating a mapping between uniform random variables on the cube and random Gaussian vectors.

In the lemma below, we consider the standard Gaussian density in $\mathbb{R}^n$ given by $p(x) = \frac{1}{(2\pi)^{n/2}} e^{-nx^2/2}$ and corresponding Gaussian measure μ. We also define

$$\Phi(z) = \frac{1}{\sqrt{2\pi}} \int_{-\infty}^{z} e^{-t^2/2} dt,$$

which is the cumulative density of a Gaussian curve.

The following Lemma was first proved in Sudakov & Tsirelson (1974), and an elementary proof was given in Bobkov et al. (1997).

Lemma 5 (Gaussian Isoperimetric Inequality). *Of all sets with the same Gaussian measure, the set with ℓ_2 ϵ-expansion of smallest measure is a half space. Furthermore, for any measurable set $\mathcal{A} \subset \mathbb{R}^n$, and scalar constant a such that $\Phi(a) = \mu[\mathcal{A}]$,*

$$\mu[\mathcal{A}(\epsilon, d_2)] \geq \Phi(a + \epsilon).$$

Using this result we can now give a proof of Lemma 3.

This function Φ maps a random *Guassian* vector $z \in N(0, I)$ onto a random *uniform* vector in the unit cube. To see why, consider a measurable subset $\mathcal{B} \subset R^n$. If μ is the Gaussian measure on $\mathbb{R}^n$ and σ is the uniform measure on the cube, then

$$\sigma[\Phi(\mathcal{B})] = \int \chi_{\Phi(\mathcal{B})}(s) d\sigma = \int \chi_{\Phi(\mathcal{B})}(\Phi(z)) \frac{1}{\det(J\Phi)} dz = \int \chi_{\mathcal{B}}(z) d\mu = \mu[\mathcal{B}].$$

Since $\frac{\partial}{\partial z_i} \Phi(z) \leq \frac{1}{\sqrt{2\pi}}$, we also have

$$\|\Phi(z) - \Phi(w)\|_p \leq \|\frac{1}{\sqrt{2\pi}}(x - w)\|_p = \frac{1}{\sqrt{2\pi}} \|z - w\|_p$$

for any $z, w \in \mathbb{R}^n$. From this, we see that for $p^* = \min(p, 2)$

$$\|\Phi(z) - \Phi(w)\|_p \leq n^{1/p^* - 1/2} \|\Phi(z) - \Phi(w)\|_2 \leq \frac{n^{1/p^*}}{\sqrt{2\pi n}} \|z - w\|_2 \tag{10}$$

where we have used the identity $\|u\|_p \leq n^{1/\min(p,2) - 1/2} \|u\|_2$.

Now, consider any set $\mathcal{A}$ in the cube, and let $\mathcal{B} = \Phi^{-1}(\mathcal{A})$. From equation 10, we see that

$$\Phi\mathcal{B}\left(\frac{\sqrt{2\pi n}}{n^{1/p^*}} \epsilon, d_2 \right) \subset \mathcal{A}(\epsilon, d_p).$$

13

It follows from equation 10 that

$$\sigma[\mathcal{A}(\epsilon, d_p)] \geq \mu\left[\mathcal{B}\left(\frac{\sqrt{2\pi n}}{n^{1/p^*}}\epsilon, d_2\right)\right].$$

Applying Lemma 5, we see that

$$\sigma[\mathcal{A}(\epsilon, d_p)] \geq \Phi(\alpha + \frac{\sqrt{2\pi n}}{n^{1/p^*}}\epsilon) \tag{11}$$

where $\alpha = \Phi^{-1}(\sigma[\mathcal{A}])$.

To obtain the simplified formula in the theorem, we use the identity

$$\frac{1}{\sqrt{2\pi}}\int_x^\infty e^{-t^2}dt < \frac{e^{-x^2}}{\sqrt{2\pi}x}$$

which is valid for $x > 0$, and can be found in Abramowitz & Stegun (1965).

B PROOF OF LEMMA 3

Our proof emulates the method of Talagrand, with minor modifications that extend the result to other ℓ_p norms. We need the following standard inequality. Proof can be found in Talagrand (1995; 1996).

Lemma 6 (Talagrand). *Consider a probability space Ω with measure μ. For $g : \Omega \to [0, 1]$, we have*

$$\int_\Omega \min\left(e^t, \frac{1}{g^\alpha}\right)d\mu \times \left(\int_\Omega g d\mu\right)^\alpha \leq \exp\left(\frac{t^2(\alpha+1)}{8\alpha}\right).$$

Our proof of Lemma 3 follows the three-step process of Talagrand illustrated in Talagrand (1995). We begin by proving the bound

$$\int e^{tf(x,\mathcal{A})}dx \leq \frac{1}{\sigma^\alpha[\mathcal{A}]}\exp\left(\frac{nt^2(\alpha+1)}{8\alpha}\right) \tag{12}$$

where $f(x, \mathcal{A}) = \min_{y \in \mathcal{A}}\sum_i |x_i - y_i|^p = d_p^p(x, \mathcal{A})$ is a measure of distance from $\mathcal{A}$ to x, and α, t are arbitrary positive constants. Once this bound is established, a Markov bound can be used to obtain the final result. Finally, constants are tuned in order to optimize the tightness of the bound.

We start by proving the bound in equation 12 using induction on the dimension. The base case for the induction is $n = 1$, and we have

$$\int e^{tf(x,\mathcal{A})}dx \leq \sigma[\mathcal{A}] + \int_{\mathcal{A}^c} e^{tf(x,\mathcal{A})}dx \leq \sigma[\mathcal{A}] + \int_{\mathcal{A}^c} 1 dx \leq \sigma[\mathcal{A}] + (1-\sigma[\mathcal{A}])e^t \leq \frac{1}{\sigma^\alpha[\mathcal{A}]}\exp\left(\frac{t^2(\alpha+1)}{8\alpha}\right).$$

We now prove the result for n dimensions using the inductive hypothesis. We can upper bound the integral by integrating over "slices" along one dimension. Let $\mathcal{A} \subset [0, 1]^n$. Define

$$\mathcal{A}_\omega = \{z \in \mathbb{R}^{n-1} \,|\, (\omega, z) \in \mathcal{A}\} \text{ and } \mathcal{B} = \{z \in \mathbb{R}^{n-1} \,|\, (\omega, z) \in \mathcal{A} \text{ for some } \omega\}.$$

Clearly, the distance from (ω, z) to $\mathcal{A}$ is at most the distance from z to $\mathcal{A}_\omega$, and so

$$\int e^{tf(x,\mathcal{A})}dx \leq \int_{\omega \in [0,1]}\int_{z \in [0,1]^{n-1}} e^{tf(z,\mathcal{A}_\omega)}dz\,dx \leq \int_{\omega \in [0,1]}\frac{1}{\sigma^\alpha[\mathcal{A}_\omega]}\exp\left(\frac{(n-1)t^2(\alpha+1)}{8\alpha}\right).$$

We also have that the distance from x to $\mathcal{A}$ is at most one unit greater than the distance from x to $\mathcal{B}$. This gives us

$$\int e^{tf(x,\mathcal{A})}dx \leq \int_{(\omega,z)\in[0,1]^n} e^{t(f(x,\mathcal{B})+1)} \leq e^t\int_{(\omega,z)\in[0,1]^n} e^{tf(x,\mathcal{B})} \leq \frac{e^t}{\sigma^\alpha[\mathcal{B}]}\exp\left(\frac{(n-1)t^2(\alpha+1)}{8\alpha}\right).$$

14

Applying equation 6 gives us

$$\int e^{tf(x,\mathcal{A})}dx \leq \int_{\omega \in [0,1]} \min\left(\frac{e^t}{\sigma^\alpha[\mathcal{B}]}\exp\left(\frac{(n-1)t^2(\alpha+1)}{8\alpha}\right), \frac{1}{\sigma^\alpha[\mathcal{A}_\omega]}\exp\left(\frac{(n-1)t^2(\alpha+1)}{8\alpha}\right)\right)$$

$$= \exp\left(\frac{(n-1)t^2(\alpha+1)}{8\alpha}\right)\frac{1}{\sigma^\alpha[\mathcal{B}]}\int_{\omega\in[0,1]}\min\left(e^t, \frac{\sigma^\alpha[\mathcal{B}]}{\sigma^\alpha[\mathcal{A}_\omega]}\right). \tag{13}$$

Now, we apply lemma 6 to equation 13 with $g(\omega) = \alpha[\mathcal{A}_\omega]/\alpha[\mathcal{B}]$ to arrive at equation 12.

The second step of the proof is to produce a Markov inequality from equation 12. For the bound in equation 12 to hold, we need

$$1 - \sigma[\mathcal{A}(\epsilon, d_p)] = \sigma\{x \mid f(x) > \epsilon^p\} \leq \frac{\int e^{tf(x,\mathcal{A})}dx}{e^{t\epsilon^p}} \leq \frac{\exp\left(\frac{nt^2(\alpha+1)}{8\alpha}\right)}{\sigma^\alpha[\mathcal{A}]e^{t\epsilon^p}}. \tag{14}$$

The third step is to optimize the bound by choosing constants. We minimize the right hand side by choosing $t = \frac{4\alpha\epsilon^p}{n(\alpha+1)}$ to get

$$1 - \sigma[\mathcal{A}(\epsilon, d_p)] \leq \frac{\exp\left(-\frac{2\alpha\epsilon^{2p}}{n(\alpha+1)}\right)}{\sigma^\alpha[\mathcal{A}]}. \tag{15}$$

Now, we can simply choose $\alpha = 1$ to get the simple bound

$$1 - \sigma[\mathcal{A}(\epsilon, d_p)] \leq \frac{\exp\left(-\epsilon^{2p}/n\right)}{\sigma[\mathcal{A}]}, \tag{16}$$

or we can choose the optimal value of $\alpha = \sqrt{\frac{2\epsilon^{2p}}{n\log(1/\sigma)}} - 1$, which optimizes the bound in the case $\epsilon^{2p} \geq \frac{n}{2}\log(1/\sigma(\mathcal{A}))$. We arrive at

$$1 - \sigma[\mathcal{A}(\epsilon, d_p)] \leq \exp\left(-\frac{2}{n}\left(\epsilon^p - \sqrt{n\log(\sigma^{-1}[\mathcal{A}])/2}\right)^2\right). \tag{17}$$

This latter bound is stronger than we need to prove Lemma 3, but it will come in handy later to prove Theorem 4.

C PROOF OF THEOREMS 2 AND 3

We combine the proofs of these results since their proofs are nearly identical. The proofs closely follow the argument of Theorem 1.

Choose a class c with $f_c \leq \frac{1}{2}$ and let $\mathcal{R} = \{x|\mathcal{C}(x) = c\}$ denote the subset of the cube lying in class c according to the classifier $\mathcal{C}$. Let $\overline{\mathcal{R}}$ be the complement, who's ℓ_p expansion is denoted $\overline{\mathcal{R}}(\epsilon; d_p)$. Because $\mathcal{R}$ covers at least half the cube, we can invoke Lemma 3. We have that

$$\text{vol}[\overline{\mathcal{R}}(\epsilon; h)] \geq 1 - \delta,$$

where

$$\delta = \begin{cases} \frac{\exp(-\pi n^{1-2/p^*}\epsilon^2)}{2\pi n^{1/2-1/p^*}}, & \text{for Theorem 2 and} \\ 2U_c\exp(-\epsilon^2/n), & \text{for Theorem 3.} \end{cases} \tag{18}$$

The set $\overline{\overline{\mathcal{R}(\epsilon; h)}}$ contains all points that are correctly classified and safe from adversarial perturbations. This region has volume at most δ, and the probability of a sample from the class distribution ρ_c lying in this region is at most $U_c\delta$. We then subtract this from 1 to obtain the mass of the class distribution lying in the "unsafe" region $\overline{\mathcal{R}}_c$.

D PROOF OF THEOREM 4

Let $\mathcal{A}$ denote the support of p_c, and suppose that this support has measure $\mathrm{vol}[\mathcal{A}] = \eta$. We want to show that, for large enough ϵ, the expansion $\mathcal{A}(\epsilon, d_p)$ is larger than half the cube. Since class c occupies less than half the cube, this would imply that $\mathcal{A}(\epsilon, d_p)$ overlaps with other classes, and so there must be data points in $\mathcal{A}$ with ϵ-adversarial examples.

We start with the case $p > 0$, where we bound $\mathcal{A}(\epsilon, d_p)$ using equation 2 of Lemma 3. To do this, we need to approximate $\Phi^{-1}(\eta)$. This can be done using the inequality

$$\Phi(\alpha) = \frac{1}{2\pi} \int_{-\infty}^{\alpha} e^{-t^2/2} dt \leq \frac{1}{2} e^{-\alpha^2/2},$$

which holds for $\alpha < 0$. Rearranging, we obtain

$$\alpha \geq -\sqrt{\log \frac{1}{4\Phi(\alpha)^2}}. \tag{19}$$

Now, if $\alpha = \Phi^{-1}(\eta)$, then $\Phi(\alpha) = \eta$, and equation 19 gives us $\alpha \geq -\sqrt{\log \frac{1}{4\eta^2}}$. Plugging this into equation 2 of Lemma 3, we get

$$\mathrm{vol}[\mathcal{A}(\epsilon, d_p)] \geq \Phi(\alpha + \epsilon) \geq \Phi\left(-\sqrt{\log \frac{1}{4\eta^2}} + \frac{\sqrt{2\pi n}}{n^{1/p^*}}\epsilon\right).$$

The quantity on the left will be greater than $\frac{1}{2}$, thus guaranteeing adversarial examples, if

$$\frac{\sqrt{2\pi n}}{n^{1/p^*}}\epsilon > \sqrt{\log \frac{1}{4\eta^2}}.$$

This can be re-arranged to obtain the desired result.

In the case $p = 0$, we need to use equation 17 from the proof of Lemma 3 in Appendix B, which we restate here

$$\mathrm{vol}[\mathcal{A}(\epsilon, d_0)] \geq 1 - \exp\left(-\frac{2}{n}\left(\epsilon - \sqrt{n \log(1/\eta)/2}\right)^2\right).$$

This bound is valid, and produces a non-vacuous guarantee of adversarial examples, if

$$\exp\left(-\frac{2}{n}\left(\epsilon - \sqrt{n \log(1/\eta)/2}\right)^2\right) < \frac{1}{2}.$$

which holds if

$$\eta > \exp\left(-\frac{2\left(\epsilon - \sqrt{n \log 2/2}\right)^2}{n}\right).$$

E PROOF OF THEOREM 5

Let $b > 1$ be an expansion factor for big MNIST. Suppose we classify b-MNIST images by downsampling them to the original 28×28 resolution (by averaging pixel blocks) and feeding them into a "back-end" low-resolution classifier. After downsampling, a $28b \times 28b$ image with perturbation of norm $b\epsilon$ becomes an 28×28 image with perturbation of norm at most ϵ. Whenever the high-resolution classifier is fooled, it is only because the back-end classifier is fooled by a perturbation of size at most ϵ, and this happens with probability at least p.

Likewise, suppose that any MNIST classifier can be fooled by perturbations of size at most ϵ with probability at least p. We can classify MNIST images by upsampling them to resolution $28b \times 28b$ and feeding them into a high-resolution classifier. After upsampling, an MNIST image with perturbation of norm ϵ becomes a $28b \times 28b$ image with perturbation of norm $b\epsilon$. The high-resolution classifier is fooled whenever the low-resolution classifier is fooled, and this happens with probability at least p.